Catalytic Properties of Pt−Ge Intermetallic Compounds in the Hydrogenation of 1,3-Butadiene

Takayuki Komatsu,* Shin-ichiro Hyodo, and Tatsuaki Yashima

Department of Chemistry, Tokyo Institute of Technology, 2-12-1 Ookayama, Meguro-ku, Tokyo 152, Japan

Received: March 28, 1997; In Final Form: May 6, 1997[⊗]

Catalytic properties of Pt−Ge intermetallic compounds, Pt_3Ge, Pt_2Ge, and PtGe, were studied for the H_2-D_2 equilibration and the hydrogenation of 1,3-butadiene. Powdered Pt, Ge, and the Pt−Ge intermetallic compounds were treated with H_2 at 873 K to reduce their surface oxidized in air. XPS spectra measured after the H_2 treatment showed the complete reduction into Pt^0 and Ge^0 and the stoichiometric surface composition for all the intermetallic compounds. The valence band XPS spectra suggested the electron transfer from Ge into Pt, which was also evidenced by the positive shift in the Ge3d XPS spectra. The activity of the intermetallic compounds for H_2-D_2 equilibration was much lower than that of pure Pt. Their low activity for the hydrogen dissociation resulted in the low activity for the hydrogenation of 1,3-butadiene. On the intermetallic compounds, no butane was formed at the initial stage of the reaction. After most of 1,3-butadiene was converted into butenes, the secondary hydrogenation of butenes into butane took place very slowly because of their intrinsically low activity for the hydrogenation of butenes. The hydrogenation with a mixture of H_2 and D_2 showed no inhibiting effect of 1,3-butadiene and 1-butene on the H_2-D_2 equilibration. Kinetic studies on the hydrogenation over Pt_3Ge revealed that the reaction rate was zero-order with respect to the partial pressure of hydrogen and first-order to that of 1,3-butadiene or 1-butene. The rate-determining step in the hydrogenation of 1,3-butadiene would be the adsorption of 1,3-butadiene. The strength of the adsorption was in the order of $H_2 \gg$ 1,3-butadiene > 1-butene on Pt_3Ge. The weaker adsorption of butenes would result in the high selectivity to butenes in the hydrogenation of 1,3-butadiene.

Introduction

Intermetallic compounds (IMC), sometimes called ordered alloys, are known to be compounds between two or more metal elements having simple stoichiometry. The most characteristic feature of IMC is their specific crystal structure different from that of their component metals, while usual alloys have the same crystal structure as that of either component metals. The specific structure sometimes gives them unique bulk properties, such as shape memory effect, hydrogen storage ability, superconductivity, and so on. Therefore, IMC have been extensively studied and utilized as new bulk materials. The surface properties of IMC, however, have not attracted much attention of scientists. In view of the catalysis, most of the investigations on IMC have dealt with so-called hydrogen storage alloys[1] because of their unique activity for hydrogen dissociation and the possibility for the stored hydrogen to participate in the reaction. Rare-earth-containing IMC are typical hydrogen storage alloys studied for the catalytic reactions. Examples are the reports on $LaNi_5$ for the synthesis of ammonia[2] and for the hydrogenation of ethylene,[3] $LaCu_5$ for the synthesis of methanol,[4] $ThNi_5$[5] and $CeAl_2$[6] for the methanation of CO, and $LaCu_2$ for the decomposition of 4-methyl-2-pentanol.[7] As the rare-earth elements are easily oxidized, the surface of their IMC could not be the genuine surface with the intermetallic structure. In the case of $LaNi_5$, the surface is covered with La_2O_3 or $La(OH)_3$ and Ni;[8] that is, the surface is similar to Ni metallic particles supported on La_2O_3.

On the other hand, supported bimetallic catalysts have been studied to enhance the activity, selectivity, and durability of their parent, monometallic catalysts. A typical example is Pt−Sn supported on alumina, which is known to be a good catalyst for the hydrocarbon reforming. In this catalyst system, Pt−Sn IMC such as $PtSn_4$, PtSn, and Pt_2Sn have been proposed to be the active species from the observation by transmission electron microscopy.[9] However, the presence of IMC has rarely been reported though the formation of an alloy is often claimed under reductive conditions.[10,11] This is because the bimetallic particles are too small for observation by X-ray diffraction. Dautzenberg et al.[12] have detected the presence of PtSn on silica-supported Pt−Sn catalysts after H_2 reduction at 623 K for 3 h, while it was detected on alumina supported one only after the reduction at 923 K for 100 h. Bacaud et al.[13] have investigated Pt−Sn/Al_2O_3 by tin Mössbauer spectroscopy and proposed the presence of various Pt−Sn IMC in addition to the Sn^{2+} and Sn^{4+} ionic species.

To clarify the catalytic properties of IMC would bring the possibility of obtaining new catalyst systems as well as provide information on the active species in bimetallic catalysts. However, the catalytic properties of IMC other than those containing rare-earth elements have never been clarified satisfactorily. Bahia and Winterbottom[14] have reported the hydrogenation of 1,3-butadiene on $ZrPd_3$. They found that $ZrPd_3$ had high selectivity for the formation of butenes compared with Pd sponge, which catalyzed the hydrogenation of butenes into butane after 1,3-butadiene was completely converted into butenes. Llorca et al.[15] have prepared PtSn IMC on silica by the interaction of *cis*-$[PtCl_2(PPh_3)_2]$ and $SnCl_2$ with the hydroxyl groups of silica and found that the supported PtSn has higher activity than usual Pt−Sn/silica for the reverse water−gas shift reaction and lactic acid formation from CO_2, ethylene, and H_2O. We have already reported on the catalytic properties of Co-containing IMC, CoGe, $CoGe_2$, CoSn, and CoAl.[16] These compounds gave much lower activity for H_2-D_2 equilibration than did pure Co. However, they catalyzed the hydrogenation

---

* Corresponding author. FAX: +81-3-5734-2758. E-mail: komatsu@chem.titech.ac.jp.

[⊗] Abstract published in *Advance ACS Abstracts,* June 15, 1997.

S1089-5647(97)01117-6 CCC: $14.00

of acetylene with a high selectivity to ethylene, while pure Co produced almost exclusively butane with a much higher rate. The unique selectivity of the Co−Ge IMC for the partial hydrogenation was found to result from their very low activity for the hydrogenation of ethylene.

The purpose of this study is to clarify the catalytic properties of Pt−Ge intermetallic compounds compared with those of parent Pt and Ge. The results together with those on Co−Ge IMC reported earlier[16] would provide further and fundamental insights into the catalytic properties of IMC consisting of transition and typical elements. Platinum is one of the most active metal catalysts, while germanium is almost inactive compared with the transition metals. The combination of these two elements, which are greatly different in the physicochemical nature, may generate unique catalytic properties as found in the case of Co−Ge IMC. The Pt−Ge binary system has six intermetallic phases, Pt_3Ge, Pt_2Ge, Pt_3Ge_2, PtGe, Pt_2Ge_3, and $PtGe_2$.[17] Among them, we used Pt_3Ge, Pt_2Ge, and PtGe because Ge-rich IMC may have a very low catalytic activity. In fact, $CoGe_2$ is less active than CoGe for the hydrogenation of acetylene.[16] The hydrogenation of 1,3-butadiene was carried out to compare the hydrogenating activity for the conjugated diene with that for the monoolefin because the geometrical environment of Pt atoms, such as the distance between Pt atoms, as well as their electronic nature, may reflect on the catalysis in the hydrogenation of two distant unsaturated bonds. In addition, Ge is also an effective additive like Sn for supported Pt reforming catalysts, and the formation of Pt−Ge alloy on alumina[18] has been reported. Therefore, the detailed study on the catalytic properties of Pt−Ge IMC might shed light also on the active species for the Pt reforming catalysts.

Experimental Section

Catalyst Preparation. Pt−Ge intermetallic compounds (IMC), Pt_3Ge, Pt_2Ge, and PtGe, were prepared by arc melting the mixture of stoichiometric amounts of platinum (Tanaka Kikinzoku Kogyo, 99.95%) and germanium (Soekawa Chemicals, 99.99%) granular metals under 400 Torr of argon. Ingots thus obtained were crushed in air and filtered into fine particles with diameters of less than 90 μm. Powders of pure Pt (Soekawa Chemicals, 99.9%) and pure Ge (Soekawa Chemicals, 99.99%) were also filtered to have diameters of less than 90 μm and used as reference catalysts.

Characterization. Temperature-programmed reduction (TPR) of IMC and their component metals, Pt and Ge, crushed in air was carried out under flowing $H_2(5\%)/N_2$ gas mixture with a TCD detector to measure the consumption of hydrogen. Trace amounts of oxygen and water in the H_2/N_2 gas mixture were removed by passing through the columns of Mn/SiO_2 and silica gel. The temperature was raised from 298 to 873 K at a heating rate of 10 K min^{-1}. The weight of the sample was 0.50 g, except for the pure Ge (0.050 g). XPS spectra of IMC, Pt, and Ge were obtained with an ESCALAB 220i spectrometer (Fisons Instruments) with an X-ray source of Mg Kα. The powdered sample was pressed into a pellet and put into a pretreatment chamber. After reduction with flowing hydrogen (101 kPa) at 873 K for 1 h, the sample was transferred into the spectrometer in vacuo to measure the spectra. Binding energies were obtained using the C1s peak (284.5 eV) as a standard.

Catalytic Reaction. Catalytic reactions were carried out using a glass circulation system connected to a quadrupole mass spectrometer (Ulvac, MASSMATE 100). Before each reaction, the sample was pretreated with 26.6 kPa of hydrogen at 873 K for 1 h followed by an evacuation at 873 K for 10 min. H_2−D_2 equilibration was performed with a mixture of H_2 (13.3 kPa) and D_2 (99 at. %, 13.3 kPa) circulated through 0.50 g (Pt_3Ge, Pt_2Ge, PtGe, and Ge) or 0.25 g (Pt) of the pretreated catalysts. The extent of the equilibration reaction was monitored by the change in the fraction of HD in hydrogen, $HD/(H_2 + HD + D_2)$, measured with the mass spectrometer. For hydrogenation reactions, a mixture of 1,3-butadiene (1,3-BD) and H_2 or 1-butene and H_2 was circulated through 0.50 g of the pretreated catalyst. Initial pressures were 6.6 kPa (1,3-BD and 1-butene) and 19.9 kPa (H_2), respectively. The extent of the reaction was monitored by the decrease in total pressure measured with a silicon diaphragm sensor, and the change in gas composition was measured with GC. H_2 and D_2 were purified by passing through the Mn/SiO_2 and silica gel columns. 1,3-BD and 1-butene were purified by repeating a freeze−pump−thaw cycle. The hydrogenation of 1,3-BD (6.6 kPa) with the mixture of H_2 (10.0 kPa) and D_2 (10.0 kPa) was carried out in a similar manner.

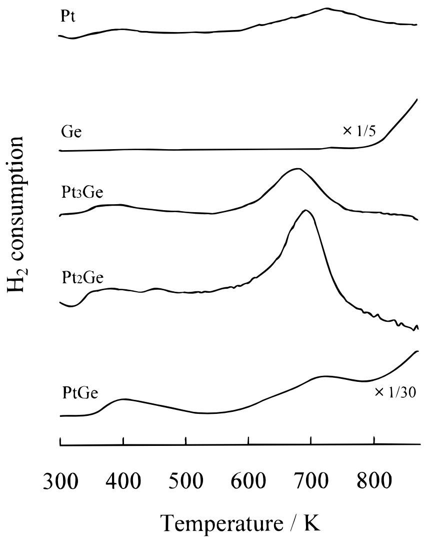

Figure 1. Temperature-programmed reduction of powdered Pt (0.50 g), Ge (0.050 g), and Pt−Ge intermetallic compounds (0.50 g).

Results and Discussion

Bulk crystal phases of the prepared Pt−Ge intermetallic compounds (IMC) were analyzed by the powder X-ray diffraction. The XRD patterns showed almost exclusively the peaks of each aimed IMC. No diffraction peaks of oxide phases were observed.

While the IMC were crushed in air to get the fine powder, their surface must be oxidized to some extent. In order to reduce the oxidized surface to obtain the genuine surface of the intermetallic phase, each IMC was treated with hydrogen at high temperatures. Temperature-programmed reduction (TPR) of the powdered IMC and their component metals was carried out to know the optimum temperature for the complete reduction without a significant sintering, which will decrease the surface area. Figure 1 shows the TPR profiles of Pt, Ge, Pt_3Ge, Pt_2Ge, and PtGe. Pure Pt powder gave two peaks at 390 and 720 K corresponding to the hydrogen consumption. As Pt is known to be easily reduced around room temperature, the 390 K peak should be assigned to the reduction of the oxidized Pt surface, though its small peak area indicates that the surface was not oxidized extensively. The 720 K peak might result from the hydrogen storage into the bulk. Pure Ge powder gave a large amount of hydrogen consumption above 800 K though only an one-tenth amount was used compared with the other samples. This indicates that the surface was extensively oxidized in air and that the reduction of the oxidized Ge, probably Ge^{4+}, needs

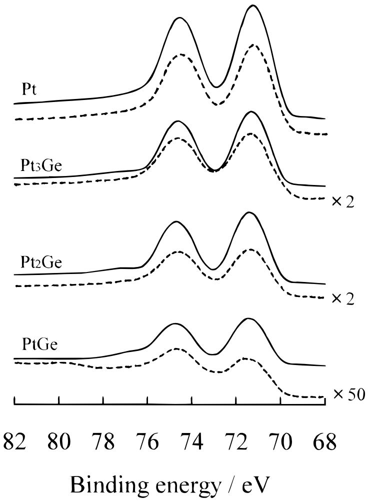

Figure 2. Pt4f XPS spectra measured before (- - -) and after (—) H_2 treatment at 873 K for 1 h.

much higher temperature than that of the Pt reduction (390 K). A small peak at 740 K might correspond to the reduction of Ge^{2+}.

The TPR of the powdered IMC gave different profiles from those of the parent Pt and Ge. Pt_3Ge and Pt_2Ge gave a broad peak at 390 K and a large peak at 670 K. It seems clear from the profile of Pt that the broad peak results from the reduction of Pt. The large peak could correspond to the reduction of Ge. However, the peak temperature was much lower than that of the pure Ge reduction. Obviously, the surface Ge atoms strongly interact with Pt, resulting in the easy reduction. As we used 0.5 g of IMC and 0.05 g of pure Ge for the TPR measurement, the amount of the oxidized Ge is small on Pt_3Ge and Pt_2Ge compared with the pure Ge. From these results, the TPR profiles of Pt_3Ge and Pt_2Ge cannot be the sum of the profiles of Pt and Ge. This could be an indication that no significant phase separation into platinum metal and germanium oxide occurs at the surface of these IMC. Pt metallic particles on some oxide supports sometimes provide a significant amount of dissociated hydrogen onto the oxide during the hydrogen treatment, accelerating the reduction of the support oxide.[19] Therefore, there remains the possibility for the phase separation if the same phenomenon occurs at the surface of IMC.

PtGe gave three peaks in its TPR profile. The reduction of Pt is represented by the peak at 390 K as in the cases of Pt_3Ge and Pt_2Ge, though its peak area was significantly large, indicating that Pt in PtGe is oxidized easier than Pt in the other Pt-rich IMC. The other two peaks at 720 and $>$870 K could arise from Ge species. The two-step reduction suggests that Ge^{2+} species exist in a comparable amount at the surface to give the 720 K peak or that Ge^{4+} species having little interaction with Pt coexists at the surface to give the peak at higher temperatures.

From the above results, we chose the pretreatment temperature of 873 K to reduce the oxidized surface, though the reduction of Ge and PtGe may not be complete at the temperature. Therefore, the oxidation state of the surface Pt and Ge atoms was next examined by X-ray photoelectron spectroscopy. Figures 2 and 3 show XPS spectra of Pt4f and Ge3d regions, respectively. The spectra were measured before and after the in situ H_2 pretreatment at 873 K for 1 h. In the case of pure Pt powder, two peaks at 71.3 and 74.6 eV were observed before the treatment. These peaks were essentially the same as $Pt4f_{7/2}$ (71.3 eV) and $Pt4f_{5/2}$ (74.6 eV) peaks of Pt foil. The binding energies and peak shape did not change after the H_2 treatment. This indicates that no appreciable oxidation occurs at the surface of Pt powdered in air, which was expected from the small TPR peak at 390 K (Figure 1). An increase in total intensity after the treatment, as was also observed for the other samples, could be ascribed to the slight sintering during the treatment at 873 K to make the surface flat to some extent.

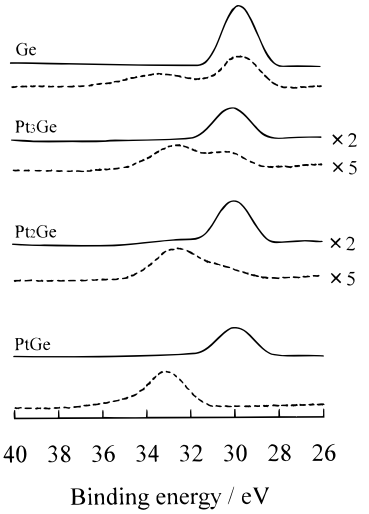

Figure 3. Ge3d XPS spectra measured before (- - -) and after (—) H_2 treatment at 873 K for 1 h.

Pure Ge powder showed two peaks at 29.6 and 33.2 eV, which correspond to Ge^0 (29.6 eV) and GeO_2 (33.0 eV), respectively. After the H_2 treatment, the peak at 33.2 eV completely disappeared, while the peak at 29.6 eV increased in intensity. It is clear that the H_2 treatment at 873 K totally reduces Ge^{4+} at the surface into Ge^0.

In the cases of Pt_3Ge and Pt_2Ge, the relative intensity of $Pt4f_{7/2}$ peak was a little weaker before the treatment. This indicates the presence of a small amount of Pt^{2+} whose $Pt4f_{7/2}$ peak overlaps the $Pt4f_{5/2}$ peak of Pt^0. The spectra after the treatment were essentially the same as the spectrum of pure Pt. Ge3d spectra gave a main peak at 32.6 eV with a smaller peak (Pt_3Ge) or a shoulder (Pt_2Ge) at 30.5 eV. The H_2 treatment eliminated the Ge^{4+} peak (32.6 eV) and gave a peak at 29.9 eV. Though this binding energy is a little higher than that of Ge^0 (29.5 eV), it is far from Ge^{2+} (ca. 31 eV). We conclude that the H_2 treatment at 873 K on Pt_3Ge and Pt_2Ge is sufficient to reduce surface Ge species oxidized in air into Ge^0.

PtGe before the treatment exhibited the different spectra from those of Pt_3Ge and Pt_2Ge. Pt4f peaks were very weak, suggesting that the surface is covered with Ge species. Moreover, the $Pt4f_{5/2}$ peak was higher than the $Pt4f_{7/2}$ peak, and no Ge^0 peak was observed, demonstrating the deep oxidation of both Pt and Ge compared with Pt_3Ge and Pt_2Ge. This deep oxidation coincides with the larger TPR peaks for PtGe than those for Pt_3Ge and Pt_2Ge (Figure 1). However, the H_2 treatment changed the spectra into almost similar ones obtained for Pt_3Ge and Pt_2Ge, with an exception that the Pt4f spectrum contained a Ge Auger peak around 77 eV. Therefore, PtGe was also found to be reduced completely by the H_2 treatment at 873 K. In the case of Pt−Ge supported on alumina,[20] H_2 treatment at 923 K reduced a part of Ge^{4+} into Ge^0, which was proposed to form Pt−Ge alloy. Though the reduction of Ge in $Pt-Ge/Al_2O_3$ was much easier than that of Ge in Ge/Al_2O_3, a strong interaction between Ge and alumina might hinder the reduction of Ge because the unsupported Ge was completely reduced into Ge^0 at 873 K in this study.

In the XPS spectra after the H_2 treatment, the binding energies of $Pt4f_{7/2}$ peaks were almost the same among pure Pt (71.3 eV) and IMC (71.3−71.4 eV), while those of Ge3d peaks were slightly shifted from pure Ge (29.6 eV) to IMC (29.9 eV). The higher Ge3d binding energy observed on IMC suggests that a

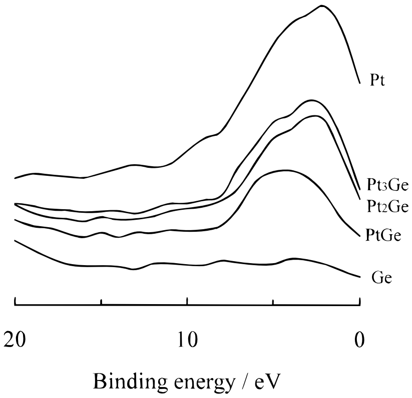

Figure 4. Valence band XPS spectra measured after H_2 treatment at 873 K for 1 h.

TABLE 1: Surface Composition of Pt−Ge Intermetallic Compounds

	Pt composition/at. %		
sample	stoichiometry	before reduction	after reduction
Pt_3Ge	75[a]	74	79
Pt_2Ge	67	62	67
PtGe	50	5	51

[a] 76−78 at. % in phase diagram.[17]

significant electron transfer from Ge to Pt occurs on IMC to lower the electron density of Ge. We measured the valence band XPS spectra to know further the electronic state in IMC (Figure 4). Pure Pt and IMC gave a peak near the Fermi level, while pure Ge did not show any significant peak. The peak near the Fermi level can be assigned to Pt5d orbitals. The peak on IMC was obviously shifted from pure Pt with increasing Pt content. This could correspond to the electron transfer from Ge into Pt, which is in agreement with the peak shift in the Ge3d spectra (Figure 3). A similar peak shift has been reviewed for the valence band spectra of many IMC, such as Ni−Al, Ni−Mg, Pd−Al, and Pd−La systems.[21] In addition to the peak shift, it is clear that the peak became narrower with Ge content. The distance between Pt atoms should be longer in IMC than that in pure Pt with fcc structure because of the dilution by Ge atoms as well as the change in the crystal structure. This results in the less overlap of Pt5d orbitals and the narrower band width.

Table 1 shows the surface composition of IMC calculated from the core level XPS spectra. In the cases of Pt_3Ge and Pt_2Ge, the surface Pt compositions were almost the same as their stoichiometric values and did not change significantly by the H_2 treatment. Therefore, we conclude that Pt_3Ge and Pt_2Ge have the genuine intermetallic phase even at their surface after the H_2 treatment at 873 K. On the other hand, PtGe exhibited very low surface Pt composition before the H_2 treatment as expected from its weak Pt spectrum (Figure 2). This surface enrichment in Ge before the reduction implies the presence of the surface Ge species having little interaction with Pt. Such a Ge species was already assumed to explain the two-step TPR profile (Figure 1). The H_2 treatment increased the Pt composition to reach the stoichiometric value. Therefore, we conclude that PtGe also has the genuine surface intermetallic phase after the H_2 treatment.

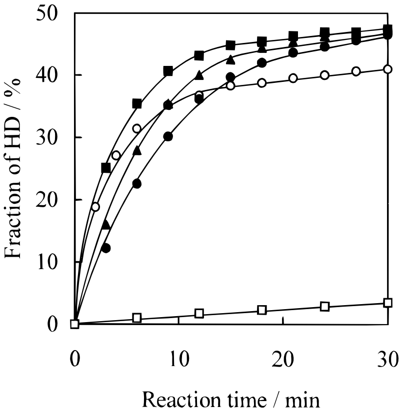

Figure 5. H_2-D_2 equilibration on Pt (○, 298 K), Ge (□, 573 K), Pt_3Ge (■, 523 K), Pt_2Ge (▲, 523 K), and PtGe (●, 573 K).

The catalytic properties of Pt−Ge IMC were first studied for H_2-D_2 equilibration. Figure 5 shows the change in the fraction of HD in gas phase with reaction time. Catalysts were pretreated with H_2 at 873 K for 1 h to obtain the specific metallic or intermetallic surface as mentioned above. On pure Pt, HD was produced readily at 298 K. However, the HD fraction was leveled off at about 40% and did not reach its equilibrium value, 47.4%, at this temperature. A significant amount of stored hydrogen during the H_2 pretreatment might result in the lower equilibrium value of the HD fraction. Pt_3Ge did not show any activity for HD formation at 298 K. It required 523 K to catalyze the reaction with a similar rate of HD formation to that obtained on Pt at 298 K. Pt_2Ge exhibited a little lower activity at the same temperature, 523 K, while higher temperature (573 K) was needed to get a comparable reaction rate on PtGe. The fraction of HD on these IMC approached its equilibrium value, 48.7% at 523 K or 48.9% at 573 K. Pure Ge powder was the least active and gave a very low rate of HD formation even at 573 K. The active site in the Pt−Ge IMC should be Pt atoms. We have already reported[16] the much lower activity of Co−Ge intermetallic compounds for the H_2-D_2 equilibration than that of pure Co.

Though we did not measure the specific surface areas of the powdered catalysts, the activity for the H_2-D_2 equilibration was found to decrease to a great extent with decreasing Pt content except for the difference between Pt_3Ge and Pt_2Ge. We can conclude that the activity of Pt−Ge IMC and their component metals for the dissociation of hydrogen is in the order of Pt $\gg$ $Pt_3Ge \geq Pt_2Ge \gg$ PtGe $\gg$ Ge. The huge difference in the activity between Pt and Pt−Ge IMC demonstrates that no phase separation into Pt and Ge particles takes place at the surface of the IMC. This again supports the regeneration of the genuine intermetallic surface by the H_2 treatment. The difference in activity might be caused by the change in the electronic state of Pt as can be seen in the valence band XPS spectra (Figure 4), because the shift of the Pt5d band to the higher binding energy makes the spectrum relatively closer to that of Au, which is much less active as a catalyst. However, the difference in the geometric circumstances around the active Pt sites may not be excluded to be the cause of the huge activity change.

Compared with Pt, the low activity of Pt−Ge IMC for the H_2-D_2 equilibration implies their different activity and selectivity for the reactions containing hydrogen, for example, hydrogenation. We have found[16] the high selectivity for the partial hydrogenation of acetylene into ethylene on Co−Ge IMC. In this study, Pt−Ge IMC were used as a catalyst for the hydrogenation of 1,3-butadiene (1,3-BD). Figure 6 shows the results obtained on pure Pt; gas phase composition against the reaction time (a) and the selectivity to each product against the conversion of 1,3-BD (b). An excess amount of H_2 was supplied for the total conversion of 1,3-BD into butane. At any reaction time, the decrease in total pressure agreed well with the consumption of H_2 calculated from the hydrogenated products. Therefore, the formation and accumulation of coke or oligomer on the surface can be neglected for the discussion on the selectivity. 1-Butene, *trans*-2-butene, *cis*-2-butene, and butane were the reaction products. The formation of butane was obvious even at the initial stage of the reaction. This is a

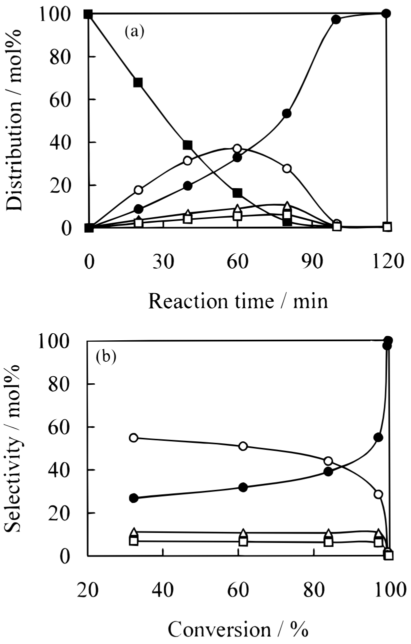

Figure 6. Gas phase composition (a) and selectivity (b) in the hydrogenation of 1,3-butadiene on Pt at 298 K. 1,3-BD (■), 1-butene (○), *trans*-2-butene (△), *cis*-2-butene (□), and butane (●).

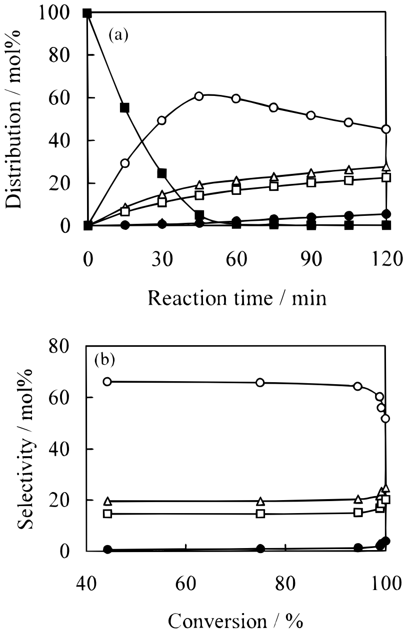

Figure 7. Gas phase composition (a) and selectivity (b) in the hydrogenation of 1,3-butadiene on Pt_3Ge at 523 K. Symbols are the same as those in Figure 6.

typical result on Pt-supported catalysts.[22,23] The rate of butane formation increased with increasing reaction time especially after most of 1,3-BD was reacted. Finally, gas phase contained exclusively butane at 120 min of the reaction time. 1-Butene was the main product in butene isomers. The isomerization of 1-butene to 2-butenes occurred very slowly; a 1-butene/2-butene ratio at 50% conversion was about 3.0, which was slightly higher than the value (1.9) obtained on Pt/Al_2O_3 at 288 K.[22] The activity of pure Ge was very low. Only 1.6% conversion was obtained at 573 K for 2 h of the reaction.

The Pt−Ge IMC gave a comparable conversion to that on Pt at 298 K when the reaction temperature was raised to 523 K and higher. Figure 7 shows the result on Pt_3Ge obtained at 523 K. Butane was not formed at the initial stage of the reaction, which is totally different from the result on Pt (Figure 6). After most of 1,3-BD was converted into butenes, butane was formed with a much slower rate than that of the initial formation of butenes. It is clear that Pt_3Ge has the high selectivity for the butene formation in the hydrogenation of 1,3-BD. The 1-butene/2-butene ratio at 50% conversion was 2.0. After 1,3-BD was totally consumed, the isomerization of 1-butene into 2-butenes gradually occurred.

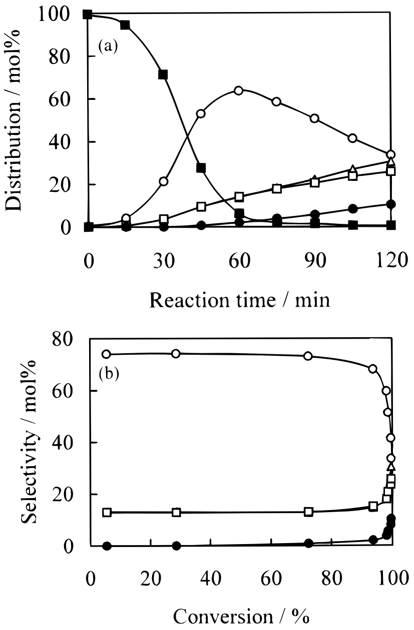

Figure 8. Gas phase composition (a) and selectivity (b) in the hydrogenation of 1,3-butadiene on Pt_2Ge at 523 K. Symbols are the same as those in Figure 6.

As shown in Figure 8, Pt_2Ge exhibited a similar tendency to Pt_3Ge at 523 K, that is, butane was scarcely formed until most of 1,3-BD was converted into butenes, though an induction period was observed for the butene formation. The rate of 1-butene isomerization after 1,3-BD conversion exceeded 95% was slightly higher, and the 1-butene/2-butene ratio was 2.9. Because the activity and selectivity of Pt_2Ge after the induction period were close to those of Pt_3Ge, a certain transformation of surface structure might occur from the genuine Pt_2Ge surface structure into a Pt_3Ge like structure during the induction period.

PtGe was less active than Pt_3Ge and Pt_2Ge. Therefore, the reaction was carried out at 573 K as shown in Figure 9. Butane was not formed significantly, and the 1-butene/2-butene ratio at 50% conversion was estimated as 3.9. In the case of Pt alloy, Bortolini and Massardier[24] have reported that when Pt was alloyed with Fe ($Pt_{80}Fe_{20}$), the activity for the hydrogenation of 1,3-BD increased and that the selectivity to butenes also increased from 58 to 89 mol % at 50% conversion. This increase in selectivity was not so evident compared with Pt−Ge IMC, where the selectivity was almost 100 mol %, though the activity decreased much by forming IMC. This difference in the effect of second element may result from the change in the Pt crystal structure in the IMC as well as the difference in the electronic nature of the second element.

From the above results, the characteristic catalysis by Pt−Ge IMC in the hydrogenation of 1,3-BD is summarized as follows compared with the pure Pt and Ge:

(1) The activity decreased in the order of $Pt \gg Pt_3Ge \geq Pt_2Ge > PtGe \gg Ge$.

(2) Very low activity for butane formation in the presence or even in the absence of 1,3-BD resulted in the high selectivity to butenes. The activity order was in good agreement with that in H_2-D_2 equilibration (Figure 5). Therefore, the low activity of Pt−Ge IMC for the 1,3-BD hydrogenation can be explained by their low activity for the dissociation of hydrogen. In order

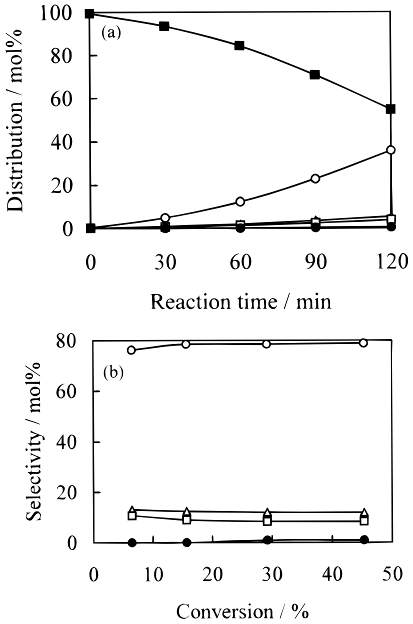

Figure 9. Gas phase composition (a) and selectivity (b) in the hydrogenation of 1,3-butadiene on PtGe at 573 K. Symbols are the same as those in Figure 6.

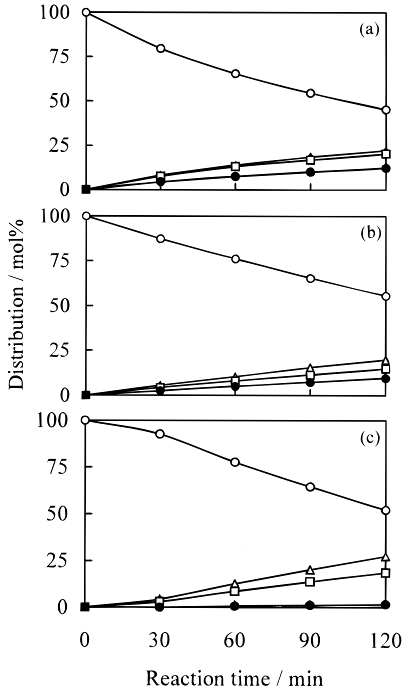

Figure 10. Gas phase composition in the hydrogenation of 1-butene on Pt_3Ge at 523 K (a), Pt_2Ge at 523 K (b), and PtGe at 573 K (c). 1-butene (○), *trans*-2-butene (△), *cis*-2-butene (□), and butane (●).

to clarify the reason for the high selectivity of Pt−Ge IMC for the butene formation, the hydrogenation of 1-butene was performed under the equivalent conditions used for the 1,3-BD hydrogenation.

On pure Pt, 1-butene was hydrogenated quickly into butane within 0.5 min at 298 K with an evolution of the heat of reaction. It is clear that Pt catalyzes the hydrogenation of 1-butene much easier than that of 1,3-BD. The high activity for the 1-butene hydrogenation must result in the simultaneous formation of butane during the 1,3-BD hydrogenation. The rate of butane formation shown in Figure 6, however, was much slower than that measured separately without 1,3-BD. The inhibiting effect of adsorbed 1,3-BD on the hydrogenation of 1-butene is obvious.

On the other hand, the rate of the 1-butene hydrogenation on Pt−Ge IMC was lower than that of the 1,3-BD hydrogenation. Figure 10 shows the results of the 1-butene hydrogenation on Pt_3Ge, Pt_2Ge, and PtGe. The comparison between the conversion rate of 1,3-BD in Figures 7, 8, or 9 and the formation rate of butane in parts a, b or c of Figure 10 clearly demonstrates the low activity of IMC for the 1-butene hydrogenation. PtGe catalyzed mainly the isomerization into 2-butenes. In the cases of Pt_3Ge and Pt_2Ge, the rate of butane formation in the 1,3-BD hydrogenation after most of 1,3-BD was converted was almost the same as that in the 1-butene hydrogenation on each catalyst. It is concluded, therefore, that the main reason for the high selectivity of IMC for the butene formation in the 1,3-BD hydrogenation is their intrinsically low activity for the butene hydrogenation, though the slight poisoning effect of coexisting 1,3-BD to retard the butane formation was apparent on Pt_3Ge and Pt_2Ge. The poisoning species could be the adsorbed 1,3-BD, because the poisoning effect was not obvious after the complete conversion of 1,3-BD. This development of activity was seen in the rate of isomerization of 1-butene into 2-butenes as well as in the rate of butane formation. Pt_2Ge did not give the induction period in the 1-butene hydrogenation (Figure 10b). The induction period observed in the 1,3-BD hydrogenation (Figure 8), therefore, could not be caused by butenes formed in the reaction but by 1,3-BD.

The difference in the activities of Pt−Ge IMC for the hydrogenation of 1,3-BD as can be seen in Figures 7a, 8a, and 9a was relatively large compared with that for the hydrogenation of 1-butene shown in Figure 10. The geometry of Pt atoms represented by the distance between the adjacent Pt atoms differs among the Pt−Ge IMC. The larger difference in their activities for the 1,3-BD hydrogenation might be an evidence for the geometrical effect because 1,3-BD usually needs two Pt sites, while 1-butene can be adsorbed on a Pt site.

For Co−Ge IMC, CoGe, and $CoGe_2$, we have reported[16] the unique catalysis for the selective formation of ethylene in the hydrogenation of acetylene comparing with the complete hydrogenation to form ethane on pure Co catalyst. A significant retardation of hydrogen dissociation by ethylene found on CoGe has been proposed to be the main reason for the selective formation of ethylene. The unique selectivity of the Pt−Ge IMC in the 1,3-BD hydrogenation may also be caused by the change in the hydrogen dissociation activity in the presence of hydrocarbons.

Figure 11 shows the hydrogenation of 1,3-BD on Pt with a mixture of H_2 and D_2 at 298 K. The fraction of HD in hydrogen (Figure 11a) increased with reaction time, but its formation rate was much lower than that without 1,3-BD (broken line) as shown in Figure 5. The strong adsorption of 1,3-BD may retard the dissociative adsorption of hydrogen. In Figure 11b, the change in 1,3-BD fraction in the hydrogenation with H_2 was also shown by the broken line using the data in Figure 6. It should be noted that the rate of the 1,3-BD conversion was lower with H_2/D_2 than that with H_2, showing the normal isotope effect on the reaction rates.

On the other hand, the HD formation was not affected by 1,3-BD on Pt_3Ge as shown in Figure 12a compared with that without 1,3-BD (broken line). The adsorption of 1,3-BD could be weaker than that of hydrogen. A slight decrease in HD fraction after 15 min of the reaction could correspond to the change in the equilibrium caused by the exchange between gas phase D_2 or HD and H in the hydrocarbons. The effect of 1-butene was also examined in a similar manner, and it was found that 1-butene did not affect the hydrogen dissociation, either. Similar effects of coexisting 1,3-BD and 1-butene were also observed on Pt_2Ge. Therefore, there must be a sufficient amount of hydrogen dissociatively adsorbed on Pt_3Ge and Pt_2Ge for the hydrogenation. The adsorption of 1,3-BD and 1-butene

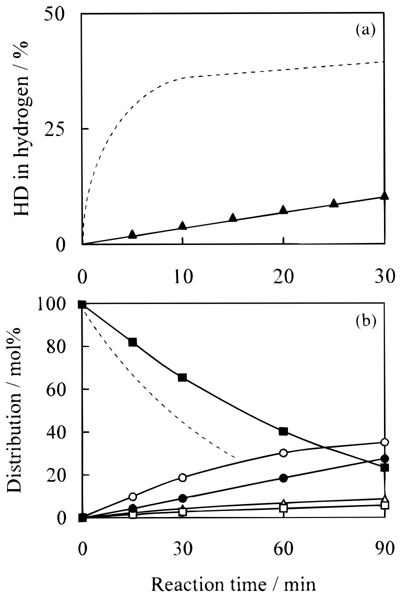

Figure 11. Hydrogenation of 1,3-butadiene with H_2/D_2 mixture on Pt at 298 K. Change in the fraction of HD in hydrogen (a) and gas phase composition (b) with reaction time. Broken lines indicate the HD formation without 1,3-BD (a) and the 1,3-BD fraction in the hydrogenation with H_2 (b). Symbols are the same as those in Figure 6.

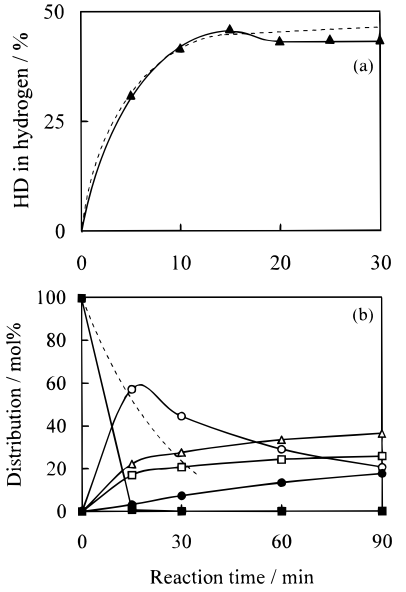

Figure 12. Hydrogenation of 1,3-butadiene with H_2/D_2 mixture on Pt_3Ge at 523 K. Change in the fraction of HD in hydrogen (a) and gas phase composition (b) with reaction time. Broken lines indicate the HD formation without 1,3-BD (a) and the 1,3-BD fraction in the hydrogenation with H_2 (b). Symbols are the same as those in Figure 6.

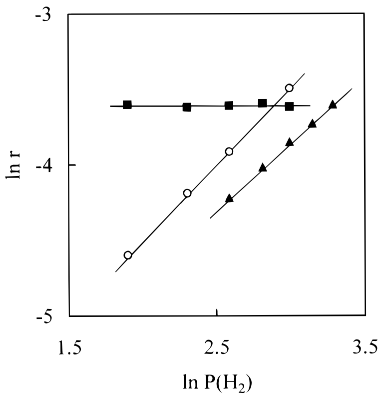

Figure 13. Dependence of the rate of 1,3-butadiene hydrogenation on the partial pressure of hydrogen for Pt at 373 K (○), Pt_3Ge at 483 K (■), and Pt_2Ge at 483 K (▲). $P(C_4H_6) = 2.7$ kPa.

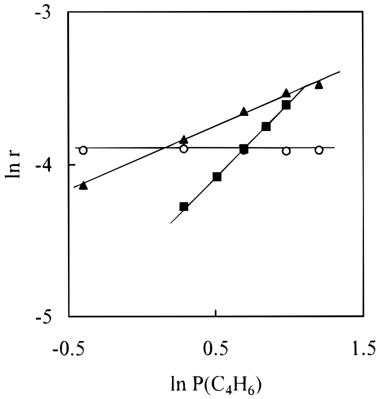

Figure 14. Dependence of the rate of 1,3-butadiene hydrogenation on the partial pressure of 1,3-butadiene for Pt at 373 K (○), Pt_3Ge at 483 K (■), and Pt_2Ge at 483 K (▲). $P(H_2) = 13.3$ kPa.

TABLE 2: Reaction Orders with Respect to the Partial Pressure of Each Reactant

	1,3-BD hydrogenation[a]		1-butene hydrogenation[b]	
catalyst	$P(H_2)$	$P(C_4H_6)$	$P(H_2)$	$P(C_4H_8)$
Pt	1.0	0		
Pt_3Ge	0	1.0	0	1.0
Pt_2Ge	0.9	0.4	0.6	0.7

[a] Reaction temperatures were 373 K for Pt and 483 K for Pt_3Ge and Pt_2Ge. Standard pressures were $P(H_2) = 13.3$ kPa and $P(C_4H_6) = 2.7$ kPa. [b] Reaction temperature was 523 K, and standard pressures were $P(H_2) = 13.3$ kPa and $P(C_4H_8) = 2.7$ kPa.

might be the rate-determining step in their hydrogenation. From Figure 12b, the inverse isotope effect was clearly observed on Pt_3Ge in the hydrogenation of 1,3-BD compared with the hydrogenation with H_2 (broken line). This will be discussed later.

The above results imply that the strength of the adsorption is the important factor governing the selectivity in the hydrogenation. Therefore, the kinetic study was carried out to know the reaction order with respect to the reactants. To obtain better reproducibility of the activity, the catalyst was used repeatedly with an evacuation at the reaction temperature for 5 min between the reactions. The weight of the catalyst was controlled to give less than 5% conversion of 1,3-BD, and the reaction temperature was selected to obtain the best reproducibility of the activity. Pt_2Ge did not show the induction period after the first run. The reaction rate thus measured was reproduced within 5% error under the same reaction conditions. Figures 13 and 14 show the dependence of the initial reaction rate on the partial pressures of H_2 and 1,3-BD, respectively, for Pt, Pt_3Ge, and Pt_2Ge. From the slope of each line, the reaction orders for each catalyst were calculated and are listed in Table 2 with the results obtained for the hydrogenation of 1-butene in a similar manner.

On Pt metal, the reaction rate was first-order to $P(H_2)$ and zero-order to $P(C_4H_6)$. This indicates that 1,3-BD is adsorbed on Pt much more strongly than H_2 and that the rate-determining step is the adsorption of H_2. This is a typical result for Pt-supported catalysts.[22] On Pt_3Ge, however, the reaction rate was zero-order to $P(H_2)$ and first-order to $P(C_4H_6)$. It is revealed that the adsorption of 1,3-BD is much weaker than that of H_2, the former step being the rate-determining step. This is the opposite result to that on Pt. In the case of the 1-butene hydrogenation, the reaction orders were zero for $P(H_2)$ and one for $P(C_4H_8)$, which indicates the weak adsorption of 1-butene as in the case of 1,3-BD. The weak adsorption of 1,3-BD and 1-butene agrees well with the negligible effect of 1,3-BD and 1-butene on the H_2-D_2 equilibration as mentioned above.

On Pt_2Ge, the reaction orders in the 1,3-BD hydrogenation were 0.9 for $P(H_2)$ and 0.4 for $P(C_4H_6)$ and those in the 1-butene hydrogenation were 0.6 for $P(H_2)$ and 0.7 for $P(C_4H_8)$. These results suggest that Pt_2Ge does not adsorb the particular molecule strongly among 1,3-BD, 1-butene, and H_2 to cover the surface active sites. Because the activity and selectivity of Pt_2Ge for the reactions tested in this study were not so much different from those of Pt_3Ge, we expected the strong adsorption of H_2 on Pt_2Ge as was observed on Pt_3Ge. The comparable strength of the adsorption of 1,3-BD and H_2 and the negligible effect of 1,3-BD on the H_2-D_2 equilibration might be explained simultaneously by the idea that the adsorption site of H_2 is different from that of 1,3-BD or that HD is formed through the adsorbed reaction intermediate in the hydrogenation of 1,3-BD in addition to the simple exchange between the dissociated H and D atoms. The different reaction orders obtained between Pt_3Ge and Pt_2Ge suggest that the surface structure and/or the electronic states of Pt are different on these IMC. Therefore, the surface transformation into the Pt_3Ge like structure proposed to explain the induction period in the 1,3-BD hydrogenation on Pt_2Ge should be excluded. The induction period might correspond to the formation of surface active species from the adsorbed 1,3-BD.

From the above results, the reaction mechanism is discussed to explain the high catalytic selectivity of Pt_3Ge for the formation of butenes in the hydrogenation of 1,3-BD. On Pt, 1,3-BD and butenes are adsorbed more strongly than H_2. The normal isotope effect observed on the rate of the 1,3-BD hydrogenation (Figure 11b) reasonably results from the difference in the zero-point energy of H_2 and D_2 because the dissociation of hydrogen is the rate-determining step. The poisoning effect of 1,3-BD on the hydrogenation of butenes is evident from the fact that butane was formed slowly in the presence of 1,3-BD (Figure 6) and that the hydrogenation of 1-butene was completed in a minute in the separate run. Therefore, the strength of the adsorption is in the order of 1,3-BD > butenes $\gg H_2$ on Pt. The strongly adsorbed 1,3-BD prevents hydrogen molecules from being adsorbed for the hydrogenation. Butenes adsorbed relatively weakly do not prevent the dissociative adsorption of hydrogen as strongly as 1,3-BD, resulting in their higher hydrogenation rate and the higher selectivity to butane in the hydrogenation of 1,3-BD.

On the surface of Pt_3Ge, 1,3-BD and 1-butene are adsorbed more weakly than H_2. The inverse isotope effect observed on the hydrogenation of 1,3-BD (Figure 12b) and 1-butene can be explained by their weak adsorption; that is, they can be adsorbed on Pt_3Ge slightly easier when the surface is covered by D instead of H because of the weaker interaction of D with the surface. From Figure 7a, the inhibiting effect of 1,3-BD was observed on the formation of butane, that is, the hydrogenation of butenes. This demonstrates the stronger adsorption of 1,3-BD than butenes on Pt_3Ge. As a result, the strength of the adsorption is in the order of $H_2 \gg$ 1,3-BD > butenes. As the rate-determining step is the adsorption of hydrocarbons, 1,3-BD has the advantage of being easily hydrogenated compared with 1-butene. During the hydrogenation of 1,3-BD, butenes formed from 1,3-BD are easily desorbed into the gas phase and can hardly be adsorbed again in the presence of hydrogen and 1,3-BD, leading to the high selectivity to butenes. After 1,3-BD is completely converted into butenes, the hydrogenation of butenes begins to occur, though the rate of this hydrogenation is very low because of the intrinsically low activity of Pt_3Ge for the butene hydrogenation.

Conclusions

The catalytic properties of Pt−Ge intermetallic compounds for the hydrogenation of 1,3-butadiene are summarized as follows compared with those of pure Pt.

(1) The activity for the hydrogenation is much lower than that of pure Pt, and it decreases with decreasing the Pt content, that is, in the order of $Pt_3Ge > Pt_2Ge >$ PtGe. Their low hydrogenation activity results from their low activity for the dissociation of hydrogen.

(2) The Pt−Ge intermetallic compounds have the high selectivity to butenes because of their lower activity for the butene hydrogenation than that for the 1,3-butadiene hydrogenation, while pure Pt has low selectivity to butenes due to its extremely high activity for the butene hydrogenation.

(3) In the case of Pt_3Ge, the lower activity for the butene hydrogenation is caused by the much stronger adsorption of H_2 and weaker adsorption of butene than that of 1,3-butadiene.

(4) The electron transfer from Ge to Pt5d orbitals as well as the difference in the geometrical environment of Pt active sites may result in the drastic change in the activity and selectivity from those of pure Pt.

The low activity for hydrogenation and hydrogen dissociation (1) and the high selectivity for partial hydrogenation (2) are similar catalytic behaviors to those of Co−Ge intermetallic compounds. This would provide general insights into the unique catalytic properties of intermetallic compounds prepared by the combination of transition and typical elements.

References and Notes

(1) Wallace, W. E. *CHEMTECH* **1982**, *12*, 752.

(2) Takeshita, T.; Wallace, W. E.; Craig, R. S. *J. Catal.* **1976**, *44*, 236.

(3) Soga, K.; Imamura, H.; Ikeda, S. *J. Phys. Chem.* **1977**, *81*, 1762.

(4) Coon, V. T.; Takeshita, T.; Wallace, W. E.; Craig, R. S. *J. Phys. Chem.* **1976**, *80*, 1878.

(5) Elattar, A.; Takeshita, T.; Wallace, W. E.; Craig, R. S. *Science* **1977**, *80*, 1093.

(6) Luengo, C. A.; Cabrera, A. L.; MacKay, H. B.; Mayple, M. B. *J. Catal.* **1977**, *47*, 1.

(7) Tkatchenko, D. B.; Branco, J.; de Matos, A. P. *J. Phys. Chem.* **1995**, *99*, 5481.

(8) Imamura, H.; Wallace, W. E. *J. Phys. Chem.* **1980**, *84*, 3145.

(9) Chojnacki, T. P.; Schmidt, L. D. *J. Catal.* **1991**, *129*, 473.

(10) Merlen, E.; Beccat, P.; Bertolini, J. C.; Delivhere, P.; Zanier, N.; Didillon, B. *J. Catal.* **1996**, *159*, 178.

(11) Coloma, F.; Escribano, A. S.; Fierro, J.-L. G.; Reinoso, F. R. *Appl. Catal. A* **1996**, *136*, 231.

(12) Dautzenberg, F. M.; Helle, J. N.; Biloen, P.; Sachtler, M. H. *J. Catal.* **1980**, *63*, 119.

(13) Bacaud, R.; Bussiere, P.; Figueras, F. *J. Catal.* **1981**, *69*, 399.

(14) Bahia, A.; Winterbottom, J. M. *J. Chem. Tech. Biotechnol.* **1994**, *60*, 305.

(15) Llorca, J.; de la Piscina, P. R.; Fierro, J.-L. G.; Sales, J.; Homs, N. *J. Catal.* **1995**, *156*, 139.

(16) Komatsu, T.; Fukui, M.; Yashima, T. 11th International Congress on Catalysis—40th Anniversary. *Stud. Surf. Sci. Catal.* **1996**, *101*, 1095.

(17) *Binary Alloy Phase Diagrams*, second edition; ASM International and National Institute of Standards and Technology: Materials Park, OH, 1990.

(18) Garetto, T. F.; Borgna, A.; Apesteguia, C. R. 11th International Congress on Catalysis—40th Anniversary. *Stud. Surf. Sci. Catal.* **1996**, *101*, 1155.

(19) Khoobier, S. *J. Phys. Chem.* **1964**, *68*, 411. Benson, J. E.; Kohn, H. W.; Boudart, M. *J. Catal.* **1966**, *5*, 307.

(20) Bouwman, R.; Biloen, P. *J. Catal.* **1977**, *48*, 209.

(21) Fuggle, J. C.; Hillebrecht, F. U.; Zeller, R.; Zolnierek, Z.; Bennett, P. A.; Freiburg, C. *Phys. Rev. B* **1983**, *27*, 2145.

(22) Bond, G. C.; Webb, G.; Wells, P. B.; Winterbottom, J. M. *J. Chem. Soc.* **1965**, 3218.

(23) Boitiaux, J. P.; Cosyns, J.; Robert, E. *Appl. Catal.* **1987**, *32*, 145.

(24) Bertolini, J. C.; Massardier, J. *Catal. Lett.* **1991**, *9*, 183.